Trends in advanced sciences and technology

Trends in Advanced Sciences and Technology

Manuscript 1021

Modeling Earthquake Catalog (1985-2022) in Northern Egypt Using Space-Time Epidemic-Type Aftershock Sequences (ETAS)

Mariam Ramadan

Amir Ismail

Amin E. Khalil

Hesham Abdelhafiez

Nouran S. Salama

ORIGINAL STUDY

Modeling Earthquake Catalog (1985–2022) in Northern Egypt Using Space-time Epidemic-type Aftershock Sequences

Mariam Ramadan Awad [a,*], Amir Ismail Abdelaziz [a,b], Amin Esmail Khalil [a], Hesham Eid Abdelhafiez [c], Nouran Salah Salama [a]

[a] Department of Geology, Faculty of Science, Helwan University, Egypt
[b] Department of Physical and Environmental Sciences, Texas A&M University-Corpus Christi, Texas, USA
[c] National Research Institute of Astronomy and Geophysics (NRIAG), Cairo, Egypt

Abstract

Earthquakes have the largest damaging effects among other natural disasters on a global scale. Efforts for reducing their effects have taken place for a long time. The prediction of earthquakes was the main target, however, the studies conducted were not successful. As a replacement, seismic hazard assessments were adopted to predict the levels of ground motion for possible future large earthquakes. This approach is probabilistic in nature and relies on the quality of the earthquake catalog. The probabilistic model adopted is built on the assumption that the events in the earthquake catalog are random Poisson's distribution, assuming that events are independent of each other. Hence, dependent events should be removed from the catalog. This algorithm is called seismic declustering. It is a step toward conducting a reliable seismic hazard analysis for the region. For this reason, the epidemic-type aftershock sequence (ETAS) model is tested to investigate its efficiency to remove dependent events from the catalog of northeastern Egypt. ETAS code is an R package for fitting the space-time ETAS model to an earthquake catalog, especially large datasets, using the stochastic declustering approach. For this purpose, an earthquake catalog for the rectangular geographical region 26°–33° N and 30°–36° E representing the northeastern part of Egypt, and period between 1985 and 2022 was extracted and processed. Applying the whole catalog data to the code results in missing the main shocks of some seismic zones of the study area. A better solution to this problem was achieved by subdividing the data in time for periods close to these main shocks. However, the Gulf of Aqaba event that took place on November 22, 1995 failed to appear as background activity. The reason for this comes from the foreshocks that preceded the main shock. For this reason, the event is added manually to the catalog.

Keywords: Dependent earthquake removal, Earthquake catalog, Epidemic-type aftershock sequence, Northeastern Egypt, Spatiotemporal earthquake distribution

1. Introduction

Egypt lies in the northeastern part of the African continent. Although earthquake activity there is considered low to moderate, even these moderate earthquakes can cause severe damage. For instance, the Cairo earthquake on October 12, 1992, with Mw = 5.9 caused severe damage because of its proximity to dense population areas with poor condition buildings. According to the tectonic framework of Egypt conducted by several researchers (e.g. Khalil & Moustafa, 1995; Meshref, 2017; Morgan, 1990; Said, 1962), the northern part of Egypt is termed as the unstable shelf including several neo-tectonic provinces such as the Gulf of Aqaba, the Gulf of Suez, the Cairo-Suez District, and the Mediterranean Sea offshore area. Besides, seismological observations showed that the northern

Received 27 June 2024; revised 28 August 2024; accepted 10 September 2024.
Available online 15 October 2024

* Corresponding author at: Department of Geology, Faculty of Science, Helwan University, Cairo 11795, Egypt.
E-mail address: mariam.ramadan@science.helwan.edu.eg (M.R. Awad).

https://doi.org/10.62537/2974-444X.1021

part of Egypt is considered more seismically active than the southern part (Fig. 1). Moreover, the northern part comprises the major proportion of the economic assets and most of the population of the country. Hence, several studies (Abdalzaher et al., 2020; Badawy, 1998; Kebeasy et al., 1981; Khalil et al., 2015; Maamoun et al., 1984; Mohamed et al., 2012) were directed toward the seismic hazard assessments to assess the vulnerability and sustainability of the region.

Seismic hazard assessments are considered as a replacement for the unsuccessful earthquake prediction efforts. For earthquake-active regions, seismic hazard assessment is optimum for the design of earthquake-resistant structures to reduce human and economic loss expected from future large earthquakes. These assessments predict the scenarios of most probable ground shaking levels that may affect buildings and strategic projects in a certain design period. Moreover, seismic hazard assessments are conducted following either deterministic or probabilistic strategy. Deterministic seismic hazard assessments consider the so-called design earthquake. Such earthquakes assume higher ground motion levels that may be considered unlikely. The technique disregards smaller events. Probabilistic hazard assessments (PSHA), however, considers several scenarios for ground motion levels taking into account all events that may affect the site under consideration.

PSHA adopts the Poisson's distribution model which assumes that events are independent of each other. Earthquake catalogs, however, are composed of independent events and dependent ones (foreshocks, aftershocks, and swarms). Thus, all dependent earthquakes must be removed from the earthquake catalog before PSHA calculations. The removal algorithm is called “declustering.”

Declustering an earthquake catalog, which is the process of removing dependent events from the earthquake catalog is mandatory for seismic hazard assessment, development of clustered seismicity

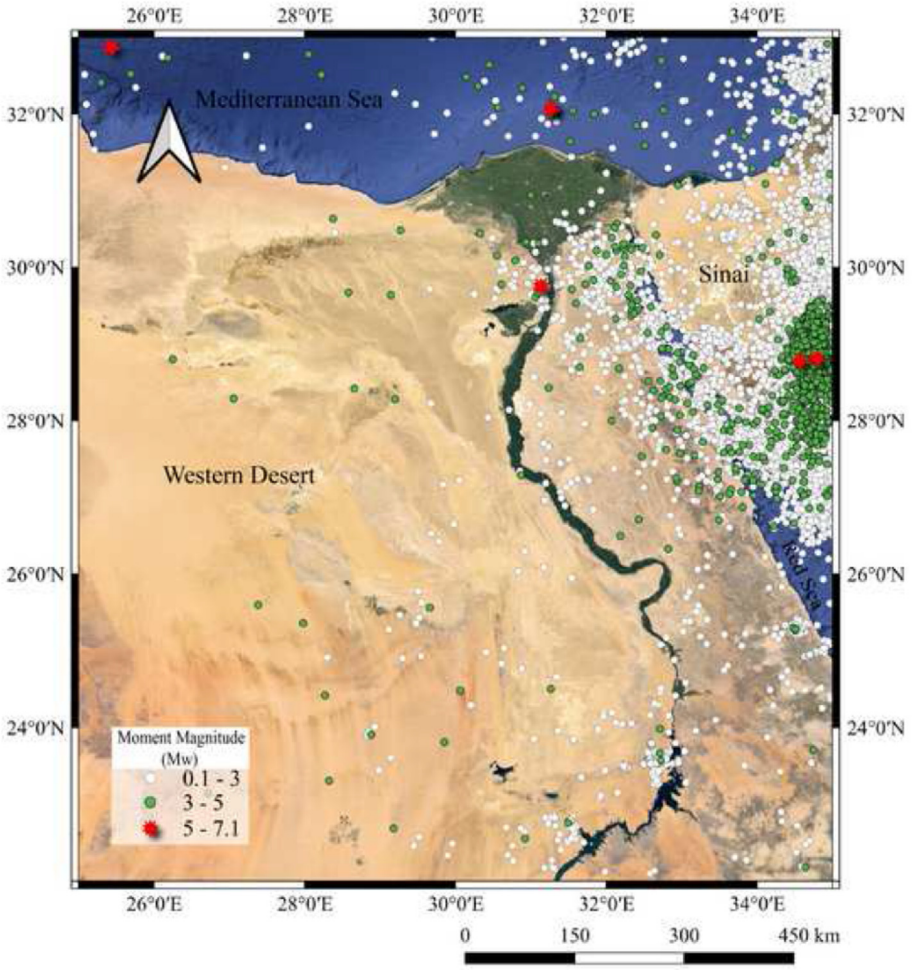

Fig. 1. Seismicity map of Egypt for the period from 1985 to 2022 (Source: International Seismological Center; European-Mediterranean Seismological Centre) (Di Giacomo and Storchak, 2016).

models, earthquake prediction research, and seismicity rate change estimation (van Stiphout et al., 2012). As discussed by van Stiphout et al. (2012), dependent earthquakes cannot be distinguished by any characteristic feature in their waveforms. Thus, they can be only distinguished based on their spatiotemporal proximity to earlier earthquakes, or by the fact that they occur at rates greater than the seismicity rate averaged over long durations (background seismicity). Therefore, to relate a dependent earthquake to a mainshock, a measure of the space–time distance between the two must be identified, and a criterion based on this measure needs to be met. Over the years, several declustering algorithms have been proposed, such as window-based methods (Gardner & Knopoff, 1974; Uhrhammer, 1986), cluster methods (Reasenberg, 1985; Savage, 1972), and probabilistic stochastic declustering approach (Kagan & Jackson, 1991; Zhuang et al., 2002, 2004, Zhuang, 2006). To the best of our knowledge, most declustering studies conducted in Egypt are based on the traditional window-based methods due to their simplicity, especially the methods of Gardner and Knopoff (1974) and Reasenberg (1985).

In this study, the stochastic approach of Zhuang et al. (2002) is evaluated as a declustering algorithm for northern Egypt earthquakes. The algorithm adopted is the epidemic-type aftershock sequence (ETAS) model. ETAS is a statistical approach that explains how each earthquake can generate its aftershocks epidemically (Davoudi et al., 2018; van Stiphout et al., 2012). This approach improves the previous traditional methods in two ways; the choice of the space–time distance is improved to best model the earthquake catalog within the limits of the ETAS model, and it gives each earthquake the probability that it is an aftershock of each preceding earthquake. Thus, all preceding earthquakes are potential mainshocks instead of binary linking an aftershock to only one mainshock. These advantages are expected to improve the PSHA studies.

2. Tectonics and seismicity of the study region

The northern part of Egypt encompasses a significant portion of the country's territory and is characterized by diverse geological formations and structures. According to Said (1990) and Abd El-Aal et al. (2020), the northern part of Egypt belongs to the Mediterranean tectonic domain, which is influenced by the interaction between the Eurasian and African plates. In addition, Egypt is bounded in the east by the transform fault movement between the African and Arabian plates (Fig. 2). This movement is attributed to the Aqaba-dead Sea transform fault. Ben-Avraham (1985) and Lyberis (1988) studied the tectonic activity of the Gulf of Aqaba and the Gulf of Suez which is affected by the relative movement between the Arabian and African plates.

The Gulf of Aqaba is believed to be a succession of NNE-SSW pull-apart basins (Garfunkel, 1981) with narrow grabens located in eastern Sinai area (Lyberis, 1988). However, the Gulf of Aqaba-Dead Sea fault system is a left-lateral movement (Badreldin et al., 2019; Freund et al., 1968, 1970; Lyberis, 1988; Quennell, 1959). The tectonic activity of the area caused several large earthquakes. The most destructive earthquake from this region was recorded on November 22, 1995, with Mw = 7.3.

The Gulf of Suez, however, extends along the western edge of the Sinai Peninsula. It was the northern termination of the Red Sea until the initiation of the Gulf of Aqaba about 19 million years ago. It was caused by the divergence movement between the African and Arabian plates. This movement is believed to have begun in the Oligocene–Miocene period (Badreldin et al., 2019; Bosworth et al., 2005, 2019; Lyberis, 1988; Said, 1990). This movement, as described by Moustafa and Khalil (2020), started as a continental rifting, which was later transformed into sea floor spreading by the continuous extension of the Red Sea. Structurally, the Gulf of Suez comprised three along-strike-linked subbasins that were separated by complex accommodation or transfer zones (Bosworth, 1985; Bosworth et al., 2019; Jarrige et al., 1990; Moustafa, 1976, 1997; Patton et al., 1994). Each of these subbasins is a mega-half graben, with the internal structure of each mega-half graben being dominated by nested, rotated fault blocks defined by sets of synthetic faults (Bosworth et al., 2019; Bosworth & McClay, 2001; Colletta et al., 1988; Patton et al., 1994; Perry & Schamel, 1990).

The Cairo-Suez District starts from Cairo and extends ~130 km eastwards through the Eastern Desert to the Gulf of Suez. The structural framework of the area can be briefly classified into three main sets; the NW Clysmic, E-W Mediterranean, and NNW fault trends as discussed by Moustafa and Abd-Allah (1992) and Hammam et al. (2020).

The area is characterized by several E-W faults with some NW-oriented faults (Moustafa and Abd-Allah, 1992; Said, 1962). The three E-W elongated belts of left-stepped, en echelon, normal faults, starting from the western-most part of the area and extending eastwards act as transfer zones between the NW-oriented normal faults parallel to and synchronous with the NW faults of the Suez rift (Moustafa and Abd-Allah, 1992). Some of these E-

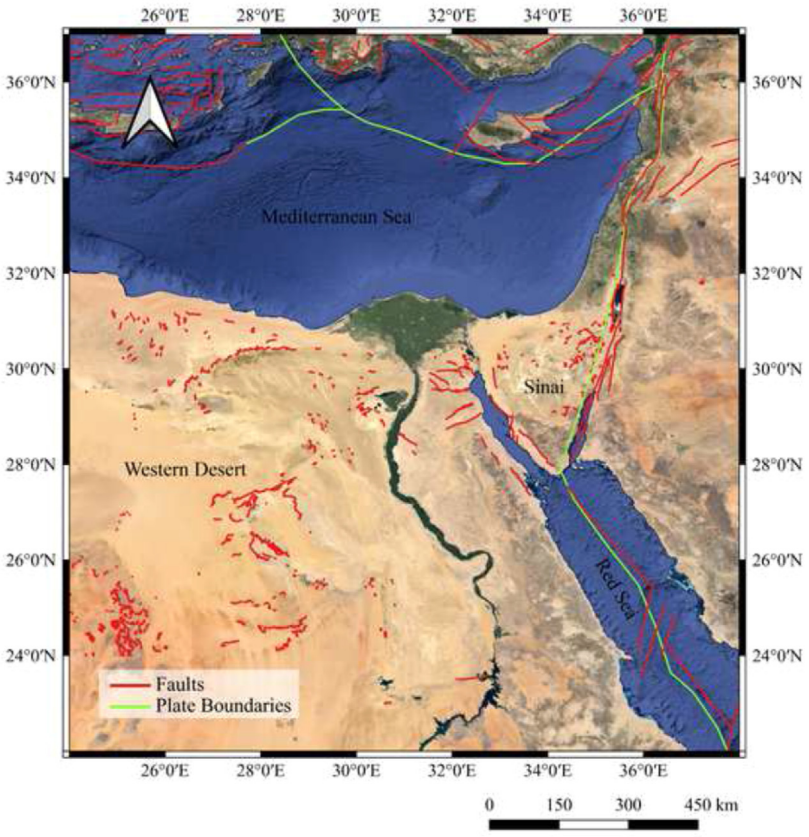

Fig. 2. Tectonic settings and active faults of Egypt and its surroundings (Sources: CASMO, GEM and National Geospatial-Intelligence Agency) (National Imagery and Mapping Agency, 1992; Heidbach et al., 2018; Styron and Pagani, 2020).

W-oriented elongated belts and NW-oriented normal faults are joined together in zigzag fault belts in the area.

Also, Egypt is affected by the earthquake activity of the Eastern Mediterranean region as it lies on the southeastern part of the Mediterranean Sea. This region represents the subduction zone between the African and Eurasian plates with the seafloor including three main arc systems as presented by McKenzie (1970, 1972); the Calabrian, Hellenic, and Cyprus arcs. The area is affected by three main fault systems: the NW-SE fault trend, the NNE-SSW fault trend, and the E-W fault trends (Mart, 1984). The subduction zones in the Mediterranean Sea caused several earthquakes, a lot of them were destructive such as the 21 July 365 CE historical strong earthquake (Ambraseys, 2009; Ott et al., 2021; Papadopoulos, 2011; Toni et al., 2024). That event caused a tsunami that destroyed most cities along the Eastern Mediterranean basin including the city of Alexandria, which was strongly affected that this event was commemorated as the "day of horror" for centuries (Ott et al., 2021). Recently, Egypt was shocked by several large earthquakes with epicenters located at the Hellenic and Cyprian arcs. Although these events were felt noticeably in North Egypt, no significant casualties were reported.

Dahshour area is another active area located to the southwest of Cairo. It has a high impact on greater Cairo, for example, the October 12, 1992 earthquake caused severe damage. It was recorded with a magnitude of Mw = 5.8 and caused the death of many people and damage to several recent and historical structures as reported by Khalil et al. (2015). The area of Dahshour, as pointed by Ml Aboud et al. (2008) and Khalil et al. (2014), is characterized by a complex structure as its surface geology does not reflect the subsurface geology but the study of Kader et al. (2013) expressed that it is highly affected by a major NNW normal fault, which has a deep extension and slightly lateral displacement and NE-conjugate faults.

3. Methodology

ETAS algorithm is used to decluster the earthquake catalog of northeast Egypt. The objective is testing the technique of removing the dependent earthquakes. For this reason, the catalog was retrieved from the regional and international

Fig. 3. Illustration of the stochastic declustering algorithm (van Stiphout et al., 2012).

datacenters. The following subsections give illustration of the algorithm and the steps followed to fit the data with ETAS model.

3.1. Stochastic declustering and epidemic-type aftershock sequence model

An earthquake catalog is considered as a chronologically ordered list of earthquake records that usually consists of date, time, magnitude, epicenter location coordinates, and focal depth. Statistically, as suggested by Ogata (1998), it is the available earthquake data presented in a space–time window. Statistical analysis can then be used to find a suitable model for the underlying earthquake process (Jalilian, 2019). Kagan and Jackson (1991) suggested that this model can be used to estimate the probabilities of future events, thus fitting an appropriate statistical model to a given earthquake catalog will be useful for seismic hazard studies.

The ETAS is one of the proposed statistical models that is based on the stochastic declustering approach. Ogata (1988, 1998) first suggested the algorithm and then was modified by Zhuang et al. (2002). The main idea of this method as described by van Stiphout et al. (2012) is an iterative approach to simultaneously estimate the background intensity, which is assumed to be a function of space but not of

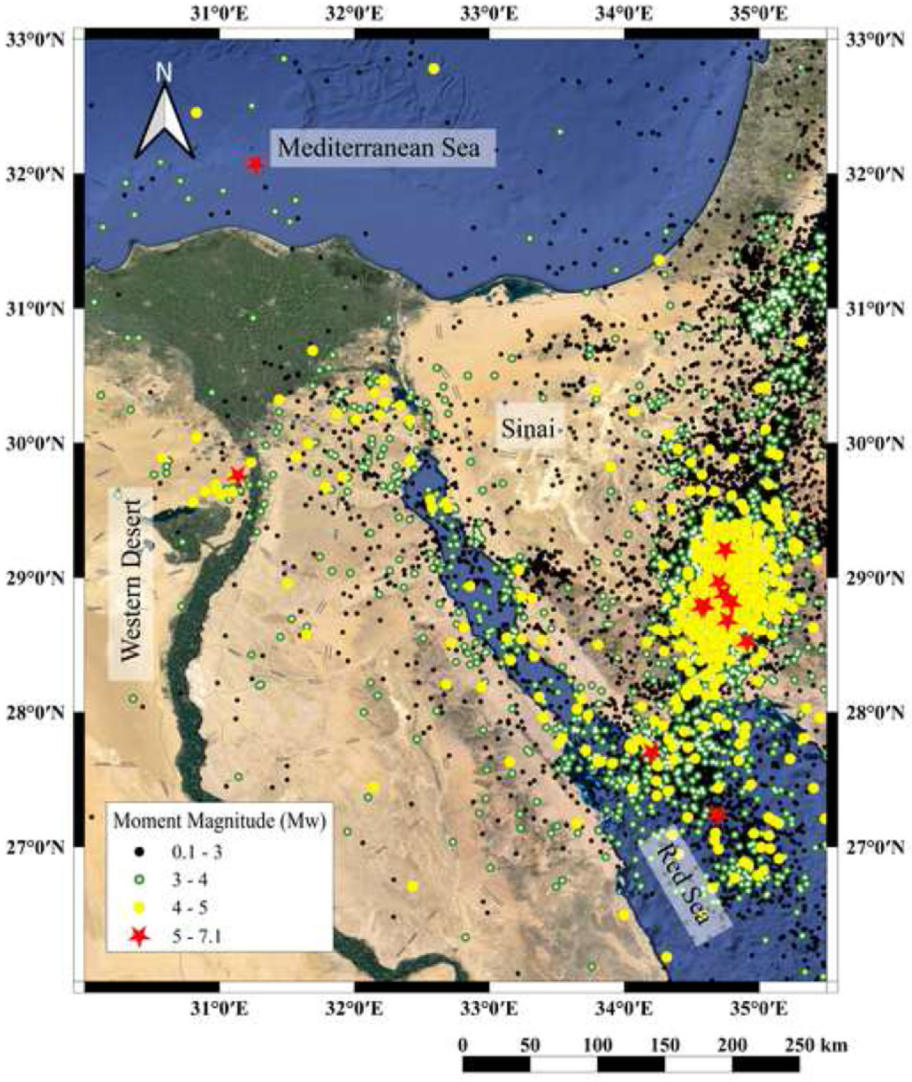

Fig. 4. Input catalog for the ETAS algorithm. ETAS, epidemic-type aftershock sequence.

time, and the parameters associated with clustering structures. Using the thinning operation for point processes, the probability of each event is a background, or a triggered event can be obtained. ETAS model can be described mathematically as follows:

$$\lambda(t,x,y) = \mu(x,y) + \sum_{\{k:t_k<t\}} k(m_k)g(t-t_k)f\left(x-x_k, y-y_k|\, m_k\right) \quad (1)$$

where μ(x, y) is the background intensity function and is assumed to be independent of time, and the functions $g(t)$ and $f(x, y|m_k)$ are, respectively, the normalized response functions of the occurrence time and the location, and the magnitude of an offspring from an ancestor of magnitude m_k. From the fact that the kth event excites a nonstationary Poisson process with intensity function $\sum_{\{k:t_k<t\}} k(m_k)g(t-t_k)f(x-x_k, y-y_k|\, m_k)$, it can be seen that $k(m_k)$ represents the expected number of offspring from an ancestor of size m_k.

Supposing that the events are numbered from 1 to N chronologically, then the probability ρ_{ij} of the jth event is triggered by the ith event can be estimated by the

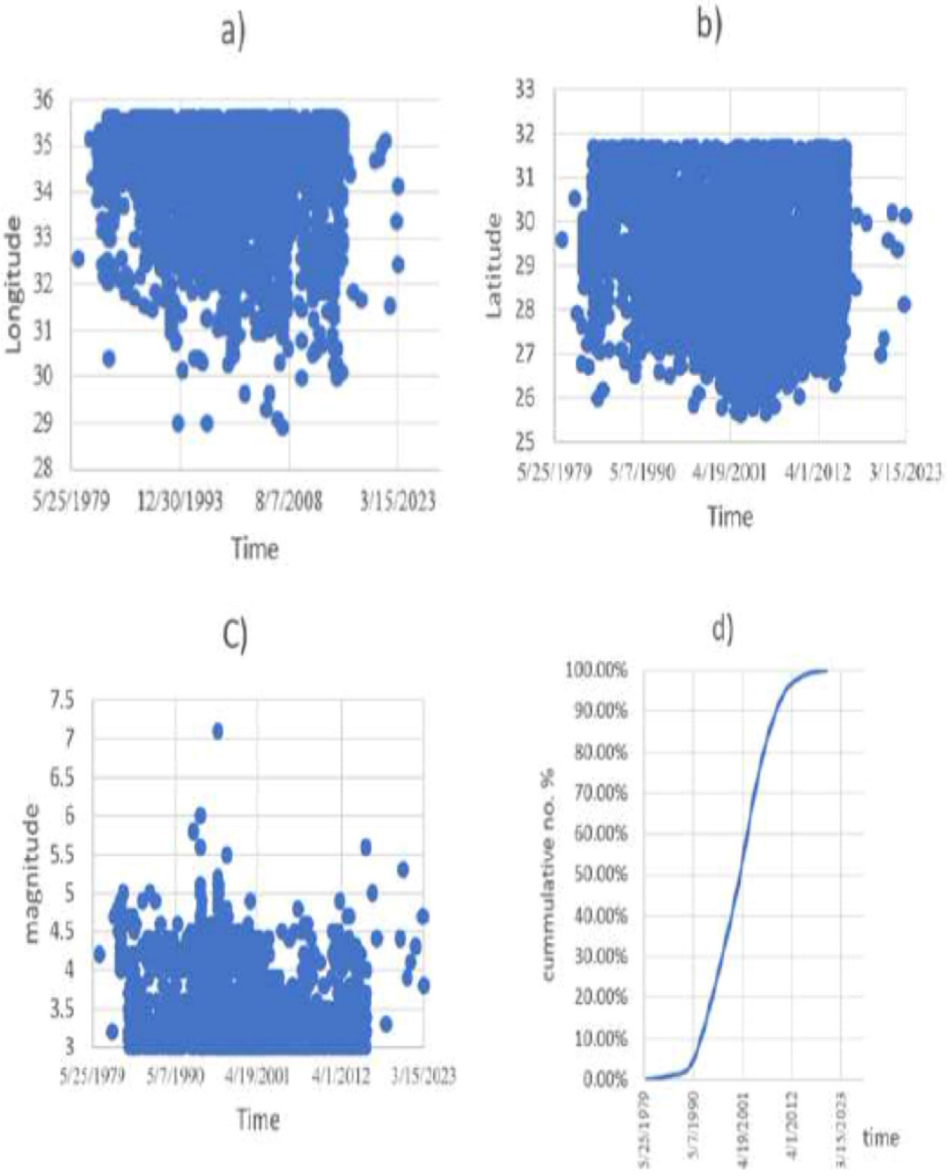

Fig. 5. Completeness and homogeneity analyses of the catalog: (a) longitude versus time, (b) latitude versus time, (c) magnitude versus time, and (d) cumulative number of events versus time.

Table 1. Subdivisions of the study periods and the magnitude threshold for each period.

Study start (day/month/year)	Study end (day/month/year)	Magnitude threshold (M_w)
01/01/1985	30/12/1990	3
01/01/1991	30/12/1993	3
01/01/1994	30/12/1995	3
01/11/1995	30/12/1999	3
01/01/2000	30/12/2022	3

$$\rho_{ij}=\begin{cases}\dfrac{k_{A,\alpha}(m_i)g_{C,P}(t_j-t_i)f_{D,\gamma,q}\left(x_j-x_i,y_j-y_i\middle|m_i\right)}{\lambda_\theta\left(t_j,x_j,y_j\middle|\lambda\mathscr{H}_{t_j}\right)}, t_j>t_i\\ 0, t_j\le t_i\end{cases} \quad (2)$$

where $\lambda(t, x, y|\lambda\mathscr{H}_t)$ is the space–time conditional intensity function, $\mathscr{H}_t=\{(t_i,x_i,y_i,m_i);t_i<t\}$ is the history of earthquakes occurrence up to time t (Ogata, 1998; Zhuang et al., 2002), $k(m_i)g(t-t_i)f(x-x_i,y-y_i|m_i)$ is the seismicity rate induced by the ith event that has already occurred (Zhuang, 2011), and θ introduces the ETAS free parameters, where θ=(μ, A, α, c, p, D, γ, q), μ is the background rate, α is the coefficient of the exponential magnitude productivity law, c is the time constant of the generalized Omori law, p is the exponent of the generalized Omori law, and q is the exponent of the spatial distribution of triggered events, and A, D, and γ are constants.

Thus, the probability that the jth earthquake is a background event is

$$\varphi_j=\frac{\mu\left(x_j,y_j\right)}{\lambda\left(t_j,x_j,y_j\right)} \quad (3)$$

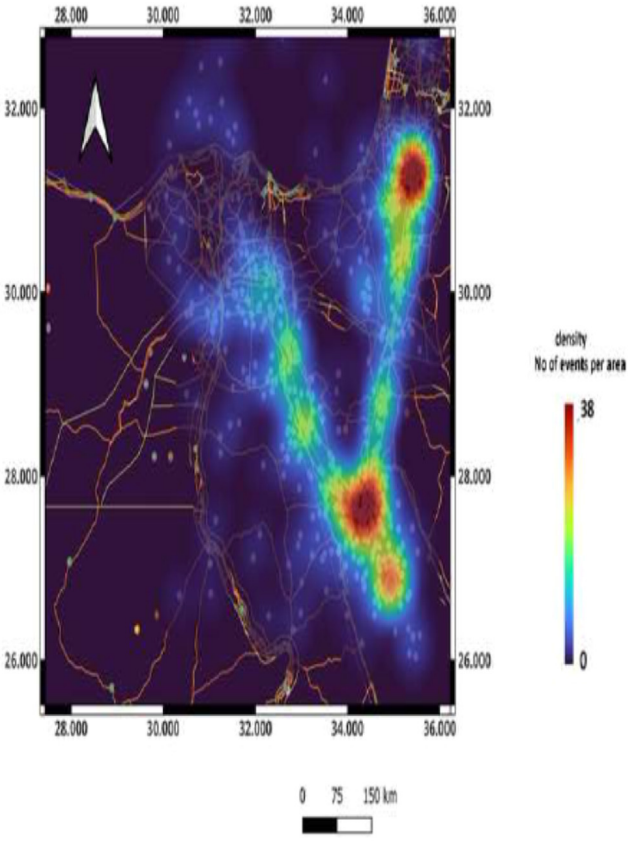

Fig. 6. Heatmap for the background seismicity.

And the probability that the jth earthquake is a triggered event is

$$\rho_j=1-\varphi_j=\sum_{i=1}^{j-1}\rho_{ij} \quad (4)$$

Consequently, as suggested by Zhuang et al. (2002) and summarized by van Stiphout et al. (2012),

Table 2. Final maximum likelihood estimates (Est.) of epidemic-type aftershock sequence model parameters and the asymptotic standard estimation errors (Std-Err) for each study period.

Period (months/years)			β	μ	A	c	α	p	D	q	γ
Study start	Study end		–	–	(event/(deg^2) × day)	(day)	(1/M)	–	(deg^2)	–	–
01/1985	12/1992	Est.	1.8126	0.7311	0.3789	0.0171	0.5255	1.1388	0.0011	1.4212	1.1168
		Std-Err	0.0123	0.0240	0.0787	0.1349	0.1188	0.0138	0.1818	0.0243	0.0956
01/1991	12/1993	Est.	1.7070	0.4069	0.3125	0.0345	1.6594	1.1270	0.0091	2.2615	0.5750
		Std-Err	0.0051	0.0345	0.0515	0.0863	0.0190	0.0087	0.0930	0.0244	0.0681
01/1994	12/1996	Est.	2.2173	0.3144	0.5734	0.0455	1.308	1.1209	0.0043	2.0549	0.5526
		Std-Err	0.0035	0.0375	0.0268	0.0600	0.013	0.0049	0.0553	0.0147	0.0399
01/1996	12/1999	Est.	2.3653	0.3773	0.5595	0.0428	1.3742	1.1015	0.0038	1.9976	0.5690
		Std-Err	0.0034	0.0269	0.0271	0.0581	0.0109	0.0041	0.0522	0.0137	0.0364
01/2000	12/2022	Est.	2.9084	0.5499	0.7714	0.0076	0.3492	1.0439	0.0008	1.4163	0.6362
		Std-Err	0.0079	0.0143	0.0718	0.0884	0.1150	0.0040	0.0787	0.0116	0.1287

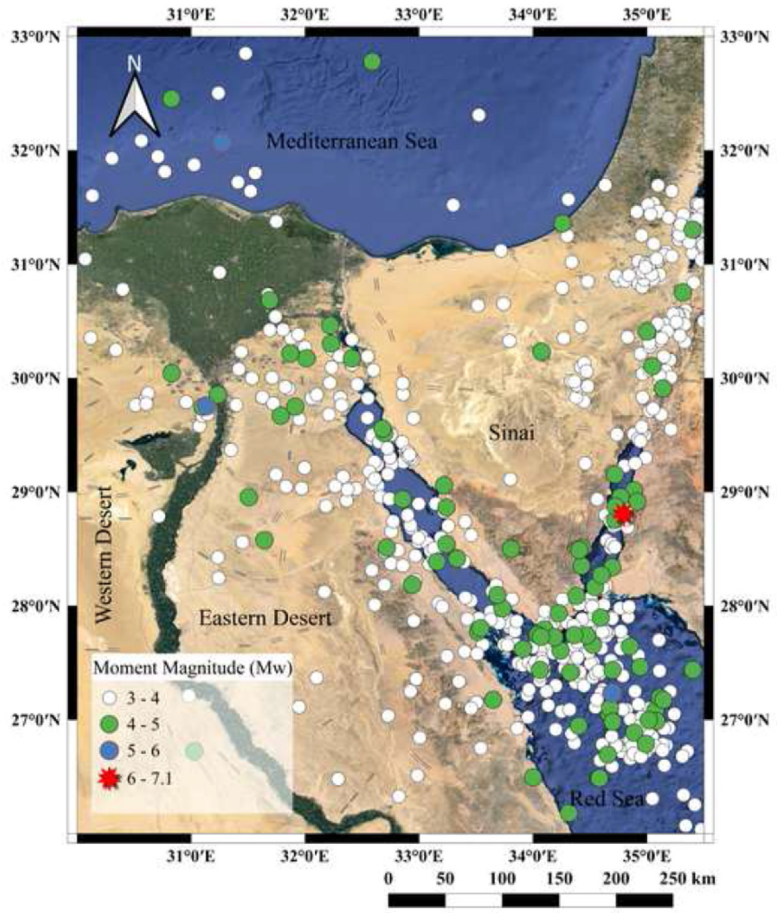

Fig. 7. Background seismicity plot for the study period from 1985 to 2022.

the following steps can be applied to the earthquake catalog to separate it into different family trees:

(1) Calculate φ_j and ρ_{ij} using equations (2) and (3), where $j = 1, 2, \ldots$. N and $i = 1,2, \ldots, j-1$, representing the total number of events.
(2) For each event j, j = 1,2, …., N, generate a random variable Uj, uniformly distributed on [0,1].
(3) For each event *j*, let

$$I_j = \min\left\{k-1 : \varphi_j + \sum_{i=1}^{k}\rho_{ij} \geq U_j \text{and } 0 \leq k < \text{j}\right\} \quad (5)$$

If $I_j = 0$, then select *j* as a background or initial event; else, set the jth event to be a direct offspring of the I_jth event.

After dividing the catalog into family trees, the initiating events in each family can be considered as background seismicity. However, the mainshocks are considered the biggest event in its family, so the biggest events in each family can be used instead of initiating events to create the background catalog (Fig. 3).

3.2. Seismicity rate and clustering coefficient estimation

The ETAS model assumes that the background seismicity rate is constant in time but varies based on location and may also have more warnings on the potential for future earthquakes (Shabani, 2022). Initial background seismicity rate was assumed using a maximum likelihood approach, then the declustering probabilities for all events were calculated from equations (2)–(4). These calculations were substituted to get better estimations of the background seismicity rates u(x, y) using weighted variable kernel estimates. These new background seismicity evaluations were used to replace initial background rates. Afterward, the clustering rate function was calculated by taking the difference

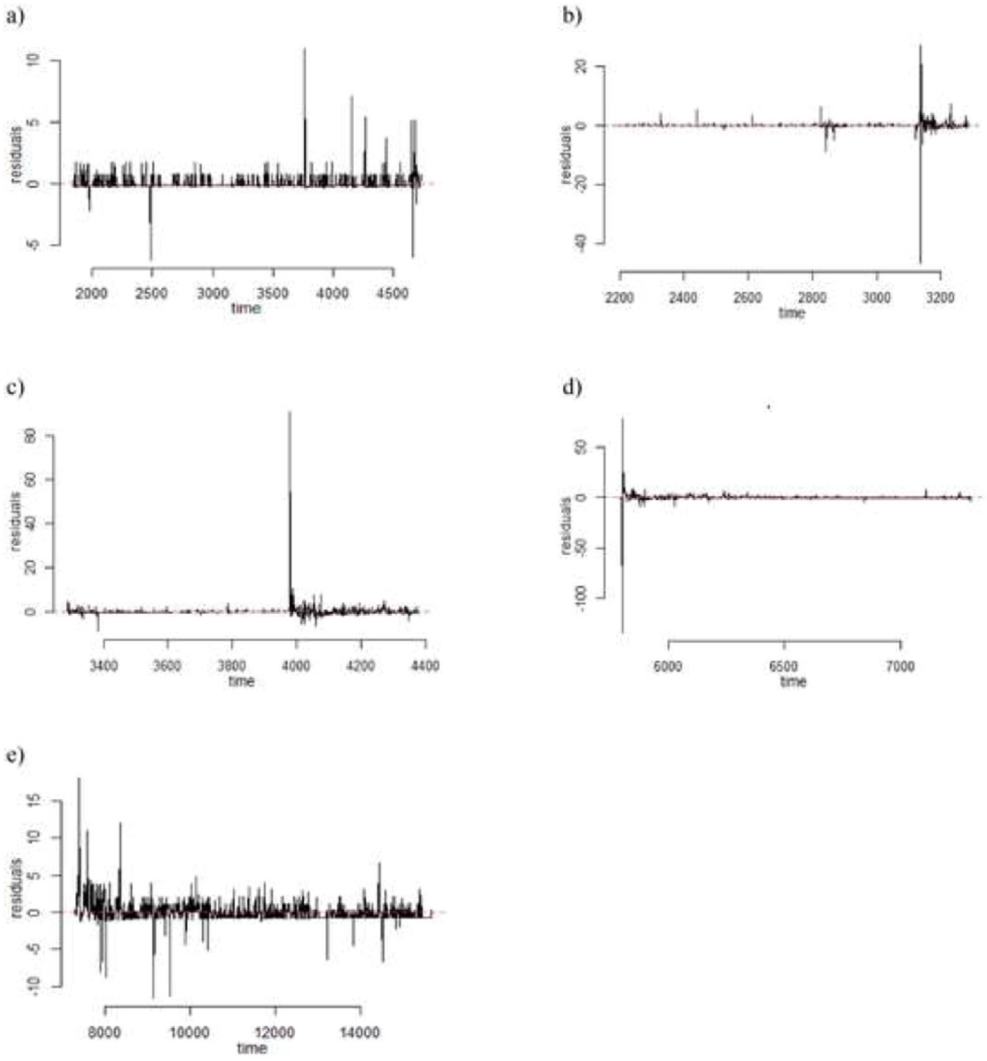

Fig. 8. Raw temporal residuals for each study period; (a) study period from 1985 to 1992. (b) study period from 1991 to 1993. (c) study period from 1994 to 1996. (d) study period from 1996 to 1999. (e) study period from 2000 to 2022.

between the total seismicity rate and the background seismicity rate.

4. Results and discussion

The earthquake catalog was downloaded from the United States Geological Survey (USGS), International Seismological Centre (ISC) and European-Mediterranean Seismological Centre (EMSC) for the rectangular geographical region 26°–33° N and 30°–36° E, representing the northeastern part of Egypt for the period between 1985 and 2022. It includes the date, time, longitude, latitude, and magnitude data. To ensure the best results, the catalog had to be processed due to many event repetitions and different magnitude types, for example, ML, MS, MB, and MW. Event duplicates were detected and removed manually, and the different magnitude types were converted and unified to MW using empirical equations.

For statistical analysis, the earthquake catalog must be complete and homogeneous, and the earthquake data quantity have a significant impact on the results. The prepared catalog consisted of ~16 500 events (Fig. 4). The relationship between magnitude and time, number of earthquakes N_t and time, longitude and time, and latitude and time (Fig. 5) were plotted to check the completeness and homogeneity of the earthquake catalog. Furthermore, it was noticed that the earthquake catalog for the targeted study period from 1985 to 2022 causes the major events to be identified as aftershocks for other background earthquakes. To overcome these issues, the input catalog is subdivided in time into smaller time span (Table 1). The completeness of earthquake data used in the current work was taken

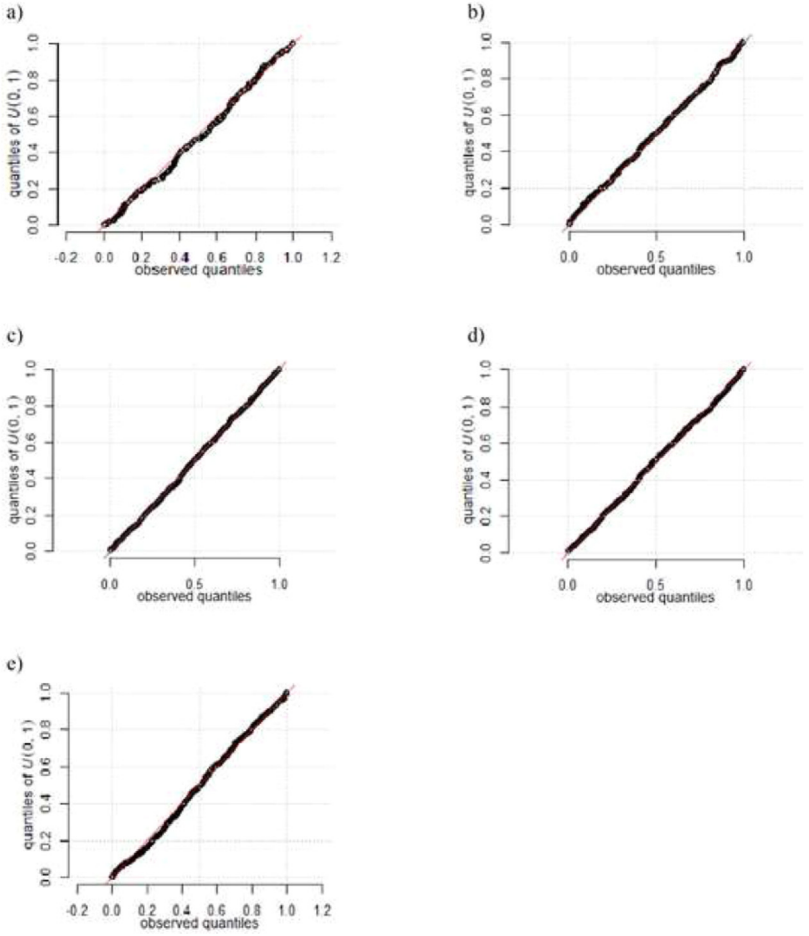

Fig. 9. Q-Q plots for each study period; (a) study period from 1985 to 1992. (b) study period from 1991 to 1993. (c) study period from 1994 to 1996. (d) study period from 1996 to 1999. (e) study period from 2000 to 2022.

from previous work (Abdalzaher et al., 2020; Khalil et al., 2015; Mohamed et al., 2012). Their work verified that the magnitude of completeness for recent Egyptian earthquake catalog is Mw = 3. The input catalog is tested against the minimum magnitude, the analysis proposed that a magnitude of M_w more than or equal to 3 is valid for the present work.

In this study, the R (Jalilian and Zhuang 2016) package ETAS from the Comprehensive R Archive Network (CRAN) was used. The ETAS parameters, background seismicity rate, and the earthquake catalog after decluster were conducted for each study subperiod. The ETAS parameters were estimated using a maximum likelihood procedure. As suggested by Ogata (1998), if there is no initial guess of ETAS parameters, the default values $\mu = N/(4\ T|S|)$, $A = 0.01$, $c = 0.01$, $\alpha = 1$, $P = 1.3$, $D = 0.01$, $q = 2$, and $\gamma = 1$ can be used. Following the iteration process suggested by Zhuang (2006), the final calculations of the free ETAS parameters were estimated after several iterations. The final maximum likelihood parameter estimations, the number of calculation iterations, and the standard estimation errors for each study period are reported in Table 2. Meanwhile, it is noticed that the asymptotic standard estimation errors of c and D parameters are larger than the parameter estimation and that may be because of the small catalog or model inadequacy.

After estimating ETAS parameters, the heatmap of the background seismicity rate for the whole study period was calculated (Fig. 6). Besides, the separate catalogs for the subperiods were collected together to get the whole background seismicity of the study period (Fig. 7). Furthermore, the goodness-of-fit of the ETAS model to the earthquake catalog was tested by residual analyses as these analyses can focus on the amount of statistical error resulting from the estimation of model parameters (Shabani, 2022).

Residual analyses include the computation and plotting of temporal residuals R^{temp} (I_j; h), spatial residuals R^{spat} (B_i; h), transformed times τ_i against j and Q-Q plots of U_j, where I_1, ….., $I_{n\ temp}$ and B_1,

….., $B_{n\ spat}$ from finite partitions of the study period $[t_{start}, t_{start} + T]$ and the geographical region S, respectively. The plotting of the temporal residuals may show possible temporal insufficiency of the fitted model; meanwhile, the plotting of the transformed times τ_i against j and the Q-Q plot of U_j show the temporal adequacy of the fitted model (Jalilian, 2019). According to Jalilian (2019), if the model is good enough then the points in the transformed time plot should approximately lie on the line where (y = x), and the Q-Q plot shows agreement between the empirical quantiles of U_j and the theoretical quantiles of a U (0, 1) distribution.

Raw temporal residuals provide insight into how well the model fits the temporal distribution of earthquakes. Raw temporal residual plots for all study subperiods show how well the model fits the catalog as the points are mostly uniformly distributed around zero except for some areas of significant spikes (Fig. 8). These areas indicate that the model underestimated the earthquake activity in these specific periods of time. Q-Q plots show normal distribution with no significant error in all study subperiods (Fig. 9), while the transformed time plots show a close fit to the theoretical (y = x) line for all study subperiods with slight to minor deviations in some areas (Fig. 10). Overall, the residual analyses verified the quality of the results of the ETAS model with slight errors in some areas, which may be due to the changes of seismicity in the study area.

Moreover, the total number of earthquakes for different magnitudes in the catalog after declustering were compared in a pivot chart for every 5 years (Fig. 11). This comparison as well as the residual analyses verified the ability of the ETAS model to decluster the Egyptian catalog.

However, while observing the declustered earthquake catalog manually, it was noticed that the ETAS model considered a few main independent earthquakes as dependent earthquakes such as the November 22, 1995, Gulf of Aqaba earthquake. This issue is believed to occur because of the presence of significant foreshocks. The influence of these foreshocks leads the mainshocks to be identified as aftershocks. Thus, it is advised to revise the resulting catalog manually as the ETAS model relies more on statistical than seismological approach.

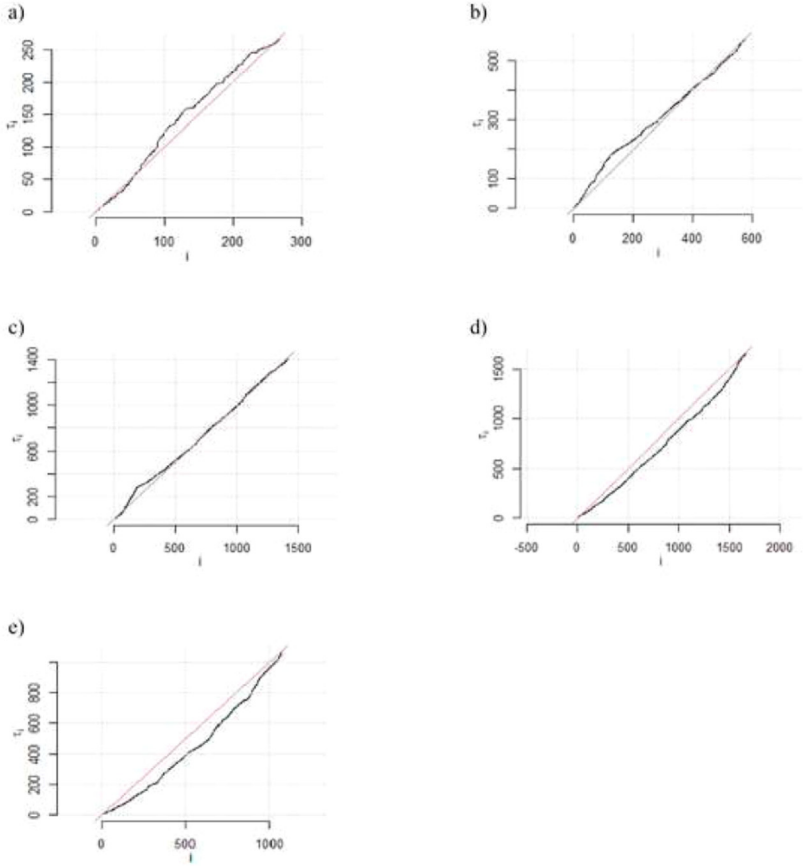

Fig. 10. Transformed times tests for each study period; (a) Study period from 1985 to 1992. (b) Study period from 1991 to 1993. (c) Study period from 1994 to 1996. (d) Study period from 1996 to 1999. (e) Study period from 2000 to 2022.

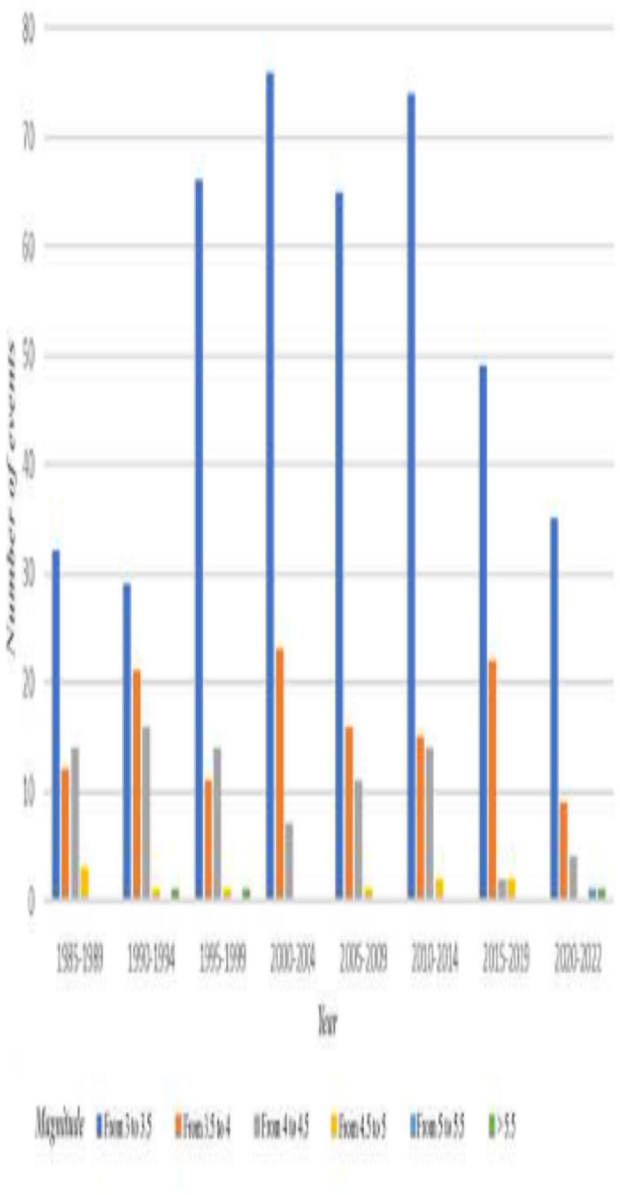

Fig. 11. Comparison between total number of earthquakes for each 5 years after declustering for different magnitudes.

4.1. Conclusion

Declustering earthquake catalogs is vital for seismic hazard assessments. The basic assumption for this is that the earthquake data must follow Poisson's distribution. Such distribution assumes that earthquakes in the catalog have no memory. Consequently, both foreshocks and aftershocks must be removed as these events are dependent on the occurrence of the mainshock. Several techniques are currently used that are based on the traditional window-based methods. These techniques are simple but may also suffer from inaccuracies, which can result in not fully removing the dependent earthquakes. Recently, the ETAS model is considered as a better candidate to do the job. The original model was introduced to fit the background seismicity model to help predict future large events. The technique was further developed to assign a probability for each event of being independent. This is a more accurate approach for removing dependent events based on spatiotemporal analysis. The present study is an attempt to test the algorithm with earthquake data that belongs to northeast Egypt. The area is characterized by both relatively high activity compared with other areas of Egypt and its strategic importance. Hence, the area is a subject for several seismic hazard assessment works. For testing purposes, data was collected from international and regional data centers. Removal of repeated events and the homogenization of magnitudes were applied before testing the technique. The earthquake catalog includes data for the period from 1985 to 2022 and it is complete for magnitude of 3.0. The ETAS technique requires a priori model parameters. From there, the algorithm iterates until reaching acceptable parameters based on certain tolerance value. However, the code may also run without specifying a priori model parameters. The present work followed both approaches. However, running the code without specifying a priori model parameters gives better solutions.

The results for the entire study period showed that several independent events were given a probability of being aftershocks. To overcome this issue, the catalog is subdivided into five subperiods around the time of known largest events. This step solved most of the problems except for the Gulf of Aqaba earthquake of November 22, 1995. The event was added manually to the background seismicity catalog. Despite the technique successfully removing all dependent events more effectively, a refinement should be added to the algorithm to solve the problem of removing some independent large events.

Funding

We confirm that all the work is done by the authors and no external funds were provided by any organization.

Author contributions

Mariam R. Awad: Data analysis, methodology, writing the first draft of the manuscript, and editing.

Amin E. Khalil: Supervision, conceptualization, validation, reviewing, and editing. **Hesham E. Abdelhafiez**: Supervision, reviewing, and editing. **Nouran S. Salama** and **Amir I. Abdelaziz**: Supervision, reviewing, and editing.

Ethics information

Ethics approval and consent to participate are not applicable.

Conflicts of interest

There are no conflicts of interest.

Acknowledgements

The authors express their gratitude to the International Seismological Centre (ISC) and the European-Mediterranean Seismological Centre (EMSC) for providing access to their comprehensive earthquake data repositories.

References

Abd El-Aal, A. E.-A. K., Hagag, W., Sakr, K., & Saleh, M. (2020). Seismicity, seismotectonics and neotectonics in Egypt. In Z. Hamimi, A. El-Barkooky, J. Martínez Frías, H. Fritz, & Y. Abd El-Rahman (Eds.), *The geology of Egypt* (pp. 375−413). Cham: Springer International Publishing.

Abdalzaher, M. S., El-Hadidy, M., Gaber, H., & Badawy, A. (2020). Seismic hazard maps of Egypt based on spatially smoothed seismicity model and recent seismotectonic models. *Journal of African Earth Sciences, 170*, Article 103894.

Ambraseys, N. (2009). *Earthquakes in the mediterranean and Middle East: A multidisciplinary study of seismicity up to 1900*. Cambridge University Press.

Badawy, A. (1998). Earthquake hazard analysis in northern Egypt. *Acta Geodaetica et Geophysica Hungarica, 33*, 341−357.

Badreldin, H., Abd el-aal, A. K., Toni, M., & El-Faragawy, K. (2019). Moment tensor inversion of small-to-moderate size local earthquakes in Egypt. *Journal of African Earth Sciences, 151*, 153−172.

Ben-Avraham, Z. (1985). Structural framework of the gulf of elat (aqaba), northern Red Sea. *Journal of Geophysical Research: Solid Earth, 90*(B1), 703−726.

Bosworth, W. (1985). Geometry of propagating continental rifts. *Nature, 316*, 625−627.

Bosworth, W., Huchon, P., & McClay, K. (2005). The Red Sea and gulf of aden basins. *Journal of African Earth Sciences, 43*, 334−378.

Bosworth, W., & McClay, K. (2001). Structural and stratigraphic evolution of the gulf of Suez rift, Egypt: A synthesis. In P. A. Ziegler, W. Cavazza, A. H. F. Robertson, & S. Crasquin-Soleau (Eds.), *Peri-tethys memoir 6: Peri-tethyan rift/wrench basins and passive margins* (Vol. 186, pp. 567−606). Mémoires du Muséum National d'Histoire Naturelle de Paris.

Bosworth, W., Taviani, M., & Rasul, N. M. (2019). Neotectonics of the Red Sea, gulf of Suez, and gulf of aqaba. In *Geological setting, palaeoenvironment and archaeology of the Red Sea* (pp. 11−35). Cham: Springer.

Colletta, B., Le Quellec, P., Letouzey, J., & Moretti, I. (1988). Longitudinal evolution of the Suez rift structure (Egypt). *Tectonophysics, 153*, 221−233.

Davoudi, N., Tavakoli, H. R., Zare, M., & Jalilian, A. (2018). Declustering of Iran earthquake catalog (1983-2017) using the epidemic-type aftershock sequence (ETAS) model. *Acta Geophysica, 66*, 1359−1373.

Di Giacomo, D., & Storchak, D. A. (2016). A scheme to set preferred magnitudes in the ISC Bulletin. *Journal of Seismology, 20*, 555−567.

Freund, R., Garfunkel, Z., Zak, I., Goldberg, M., Weissbrod, T., & Derin, B. (1970). The shear along the Dead Sea rift. *Philosophic Trans R Soc London Series A Math Phys Sci, 267*, 107−130.

Freund, R., Zak, E., & Garfunkel, Z. (1968). Age and rate of the sinistral movement along the Dead Sea rift. *Nature, 220*, 253−255.

Gardner, J. K., & Knopoff, L. (1974). Is the sequence of earthquakes in Southern California, with aftershocks removed, Poissonian? *Bulletin of the Seismological Society of America, 64*, 1363−1367.

Garfunkel, Z. (1981). Internal structure of the Dead Sea leaky transform (rift) in relation to place kinematics. *Tectonophysics, 80*, 81−108.

Hammam, A., Gaber, A., Abdelwahed, M., & Hammed, M. (2020). Geological mapping of the Central Cairo-Suez District of Egypt, using space-borne optical and radar dataset. *The Egyptian Journal of Remote Sensing and Space Science, 23*, 275−285.

Heidbach, O., Rajabi, M., Cui, X., Fuchs, K., Müller, B., Reinecker, J., et al. (2018). The World Stress Map database release 2016: Crustal stress pattern across scales. *Tectonophysics, 744*, 484−498.

International Seismological Centre, (2016). On-line bulletin. https://doi.org/10.31905/D808B830.

Jalilian, A. (2019). Etas: an R package for fitting the space-time ETAS model to earthquake data. *Journal of Statistical Software, 88*, 1−39.

Jalilian, A., & Zhuang, J. (2016). *ETAS: modeling earthquake data using ETAS model. R package version 0.2*.

Jarrige, J. J., Ott d'Estevou, P., Burollet, P. F., Montenat, C., Prat, P., Richert, J. P., & Thiriet, J. P. (1990). The multistage tectonic evolution of the Gulf of Suez and northern Red Sea continental rift from field observations. *Tectonics, 9*, 441−465.

Kader, A. K., Kordik, P., Khalil, A., Mekkawi, M., El-Bohoty, M., & Rabeh, T. (2013). Interpretation of geophysical data at El Fayoum-Dahshour Area, Egypt using three dimensional models. *Arabian Journal for Science and Engineering, 38*, 1769−1784.

Kagan, Y., & Jackson, D. (1991). Long-term earthquake clustering. *Geophysical Journal International, 104*, 117−133.

Kebeasy, R., Maamoun, M., & Albert, R. (1981). Earthquake activity and earthquake risk around the Alexandria area in Egypt. *Acta Geophys Polonica, 29*, 37−48.

Khalil, A. E., Deif, A., & Hafiez, H. A. (2015). Seismic hazard assessments at Islamic Cairo, Egypt. *Journal of African Earth Sciences, 112*, 287−298.

Khalil, M., & Moustafa, A. R. (1995). Tectonic framework of northeast Egypt and its bearing on hydrocarbon exploration. *The American Association of Petroleum Geologists Bulletin, 79*, 1409−1423.

Khalil, A., Toni, M., Hassoup, A., & Mansour, K. (2014). Analysis of aeromagnetic data for interpretation of seismicity at Fayoum-Cairo area, Egypt. *Earth Sciences Research Journal, 18*, 7−13.

Lyberis, N. (1988). Tectonic evolution of the gulf of Suez and the gulf of aqaba. *Tectonophysics, 153*, 209−220.

Maamoun, M., Megahed, A., & Allam, A. (1984). Seismicity of Egypt. *Bulletin of the Helwan Institute of Astronomy & Geophysics, 4*, 109−160.

Mart, Y. (1984). The tectonic regime of the southeastern Mediterranean continental margin. *Marine Geology, 55*, 365−386.

McKenzie, D. P. (1970). Plate tectonics of the Mediterranean region. *Nature, 226*, 239−243.

McKenzie, D. P. (1972). Active tectonics of the Mediterranean region. *Geophysical Journal International, 30*, 109–185.
Meshref, W. (2017). In , *Volume X. Tectonic framework of Egypt. Geol Egypt, Routledge* (pp. 113–155).
Ml Aboud, E., Mekkawi, M., Khalil, A., Massoud, U., & Soliman, M. (2008). Reinterpretation of magnetic data of dahshour area reveals major faults beneath and cross the Nile River, Cairo area. *NRIAG Journal of Geophysics, Special Issue*, 211–218.
Mohamed, A. E. E. A., El-Hadidy, M., Deif, A., & Abou Elenean, K. (2012). Seismic hazard studies in Egypt. *NRIAG Journal of Astronomy and Geophysics, 1*, 119–140.
Morgan, P. (1990). Egypt in the framework of global tectonics. In , *Volume X. Geology Egypt. Rotterdam* (pp. 91–111).
Moustafa, A. M. (1976). Block faulting of the gulf of Suez. In , *Vol. 19. 5th Egyptian general petroleum organization exploration seminar. Cairo*. Cairo: Egyptian General Petroleum Corporation.
Moustafa, A. R. (1997). Controls on the development and evolution of transfer zones: The influence of basement structure and sedimentary thickness in the Suez rift and Red Sea. *Journal of Structural Geology, 19*, 755–768.
Moustafa, A. R., & Abd-Allah, A. M. (1992). Transfer zones with en-echelon faulting at the northern end of the Suez rift. *Tectonics, 11*, 499–506.
Moustafa, A. R., & Khalil, S. M. (2020). Structural setting and tectonic evolution of the gulf of Suez, NW Red Sea and gulf of aqaba rift systems. *Geology Egypt* (Volume XXVI, 295–342.
National Imagery and Mapping Agency (now National Geospatial-Intelligence Agency). (1992). *DCW physiographic features, lines. [Shapefile]*. The National Geospatial-Intelligence Agency is a combat support agency within the United States.
Ogata, Y. (1988). Statistical models for earthquake occurrences and residual analysis for point processes. *Journal of the American Statistical Association, 83*, 9–27.
Ogata, Y. (1998). Space-time point-process models for earthquake occurrences. *Annals of the Institute of Statistical Mathematics, 50*, 379–402.
Ott, R. F., Wegmann, K. W., Gallen, S. F., Pazzaglia, F. J., Brandon, M. T., Ueda, K., & Fassoulas, C. (2021). Reassessing Eastern Mediterranean tectonics and earthquake hazard from the 365 CE earthquake. *AGU Advances, 2*, Article e2020AV000315.
Papadopoulos, G. A. (2011). *A seismic history of Crete: Earthquakes and tsunamis, 2000 B.C.–A.D* (Vol. 415). Athens, Greece: Ocelotos Publ.
Patton, T. L., Moustafa, A. R., Nelson, R. A., & Abdine, S. A. (1994). Tectonic evolution and structural setting of the Suez Rift. In S. M. Landon (Ed.), *Interior rift basins* (Vol. 59, pp. 7–55). Am Assoc PetrolGeol Memoire.
Perry, S. K., & Schamel, S. (1990). The role of low-angle normal faulting and isostatic response in the evolution of the Suez rift, Egypt. *Tectonophysics, 174*, 159–173.
Quennell, A. M. (1959). The structural and geomorphic evolution of the Dead Sea Rift. *Quarterly Journal of the Geological Society, 114*, 1–24.
Reasenberg, P. (1985). Second-order moment of central California seismicity, 1969-1982. *Journal of Geophysical Research: Solid Earth, 90*, 5479–5495.
Said, R. (1962). Tectonic framework of Egypt. In *The geology of Egypt* (pp. 28–44). Amsterdam: Elsevier.
Said, R. (1990). *The geology of Egypt*. A. A. Balkema.
Savage, W. U. (1972). Microearthquake clustering near fairview peak, Nevada, and in the Nevada seismic zone. *Journal of Geophysical Research, 77*, 7049–7056.
Shabani, E. (2022). *Modeling earthquake data using ETAS model to forecast aftershock subsequences applying different parameterizations in Kermanshah Region, Iran*. https://doi.org/10.21203/rs.3.rs-1996634/v1
Styron, R., & Pagani, M. (2020). The GEM global active faults database. *Earthquake Spectra, 36*(1_suppl), 160–180.
Toni, M., Badreldin, H., & El Fellah, Y. (2024). Seismicity and seismotectonic of North Africa: An updated review. In , *Volume XXV. The Geology of North Africa* (pp. 529–555).
Uhrhammer, R. A. (1986). Characteristics of northern and central California seismicity. *Earthquake Notes, 57*, 21.
van Stiphout, T., Zhuang, J., & Marsan, D. (2012). Seismicity declustering. *Community Online Resource for Statistical Seismicity Analysis, 10*, 1–25.
Zhuang, J. (2006). Multi-dimensional second-order residual analysis of space-time point processes and its applications in modelling earthquake data. *Journal of the Royal Statistical Society, 68*, 635–653.
Zhuang, J. (2011). Next-day earthquake forecasts for the Japan region generated by the ETAS model. *Earth Planets and Space, 63*, 207–216.
Zhuang, J., Ogata, Y., & Vere-Jones, D. (2002). Stochastic declustering of space-time earthquake occurrences. *Journal of the American Statistical Association, 97*, 369–380.
Zhuang, J., Ogata, Y., & Vere-Jones, D. (2004). Analyzing earthquake clustering features by using stochastic reconstruction. *Journal of Geophysical Research: Solid Earth, 109*, Article B05301.